Poisson's ratio analysis and reflection tomography

E. Menyoli and D. Gajewski[1]

ABSTRACT

Depth imaging of multi-component dataset provides a tool for estimating elastic parameters (v_p, v_s, ρ and v_p/v_s) in complex media. This paper, introduces a method of determining shear wave velocities and velocity ratio in a postmigrated domain after doing Poisson's ratio analysis (PRA). Raypaths are traced through an initial Poisson's ratio funtion and are used in combination with depth deviations in the postmigrated domain to compute Poisson's ratio perturbations. The perturbations are added to the initial Poisson's ratio function to obtain the updated Poisson's ratio. The traveltime of the CRP rays to and from the reflection point and the horizontal components of the slowness are used to constrain the raypath when parameters of the reference Poisson's ratio function are perturbed. The Poisson's ratio model is corrected by an iterative optimization technique that minimizes discrepancies in raypath. The optimization scheme is a conjugate-gradient method, where the gradient operator linearly relates perturbations in Poisson's ratio to changes in reflector positions. This includes a tomographic approach in estimating Poisson's ratios. Having the correct Poisson's ratio the shear velocity model is directly computed. We assume here that the depth model is known from previous P-wave velocity/depth analysis implying also that the wave conversion occured at the same interface as the P-wave reflection. The methodology described here has been applied to a 2D synthetic dataset but is also applicable in a 3D isotropic medium.

INTRODUCTION

The Poisson's ratio of sediments and rocks has been of special interest in seismology and oil-exploration. It can be determined from the ratio of compressional wave velocity v_p to shear wave velocity v_s. The presence of gas in the pore space of a rock layer causes a remarkable drop in the v_p/v_s ratio which leads to a decrease in the Poisson's ratio. Therefore an analysis of Poisson's ratio is vital as hydrocarbon

---

[1]**email:** menyoli@dkrz.de

indicator.

To extract elastic parameters of sediments and rocks elastic imaging is performed. On the other hand, depth imaging of elastic waves (multi-component data) is complicated due to the need to develop a consistent velocity/depth model for both P- and S-waves. Here a method for estimating and optimizing shear wave interval velocities is presented after performing velocity ratio analysis (Poisson's ratio analysis) and iterative tomography on converted waves (C-waves). In the past, two main approaches have been proposed to perform migration velocity analysis after migration and before stacking for monotypic waves: depth focusing analysis (DFA) (MacKay and Abma, 1992; Jeannot et al., 1986) and residual wavefront curvature analysis (RCA) (Al-Yahya, 1989; Deregowski, 1990; Liu and Bleistein, 1995). The methods of the above mentioned authors did not include tomographic updates. Other authors e.g. (Bishop et al., 1985), (Stork, 1992), (Kosloff et al., 1996) used migration tomography to determine the velocity/depth model for monotypic waves. The method presented here uses the residual wavefront curvature analysis and depth misfit in tomography for converted waves. More specifically, this method interprets events in depth migrated common shot sections or common offset sections, and uses the result of their interpretation to update the Poisson's ratio model and shear velocity model. No depth updating is done since the depth structure is assumed to be given from P-wave analysis. The method is useful in areas with complex geology (strong laterally variant Poisson's ratio and velocity ratio), especially in regions where the geology is dominated by salt intrusions. These regions are important for oil exploration because the impermeable salt boundaries for incident P-waves (S-wave) often serve as traps where hydrocarbons accumulate. Also at these boundaries strong wave conversion do occur allowing S-waves (P-waves) to penetrate for subsalt illumination.

Poisson's ratio analysis and velocity analysis in the premigrated domain (i.e. reflection tomography) rely on the same information in the data: energy transmitted through the velocity variations and reflected back to the surface from the underlying reflectors. In an ideal case, if a velocity field matches the data in prestack domain, it will also match it in poststack domain. In a reflection survey, each point on a reflector is generally illuminated by the data recorded from several shots, giving redundant images of the subsurface (see Figure 1). The number of fold is a measure of this redundancy. The figure is a schematic illustration of common reflection point gathers for converted waves from five different shot positions. When the prestack data is migrated to its point of reflection, there will be multiple images of that reflector, which are summed to produce the final migrated section.

If the correct Poisson's ratio (velocity models for both P and S-waves) are used in a prestack depth migration, these multiple images are identical and improve signal/noise on summing. The process of Poisson's ratio analysis is to alter the Poisson's ratio
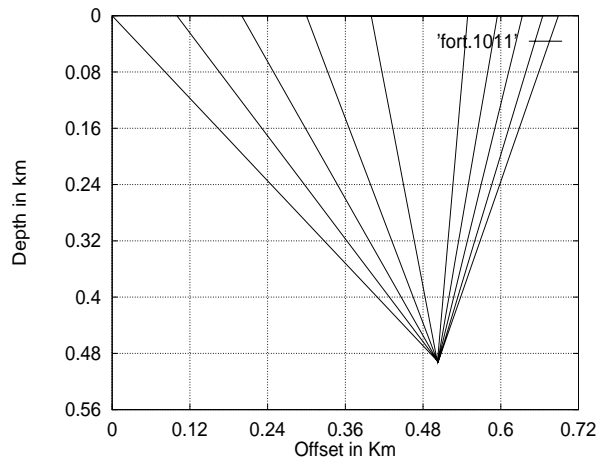
Figure 1: Rays illustrating common reflection point gathers (CRP) for converted waves. The initial model is discretized and the CRP rays are traced from source to reciever locations.

field so that these multiple images are more identical and produce a better summation. Moreover, the knowledge of Poisson's ratio is an important hydrocarbon indicator.

Analysis of properties of common reflection point (CRP) gathers or common image gathers (CIG) allows us to develop an iterative tomographic algorithm to estimate the interval Poisson's ratio directly. When lateral variation of Poisson's ratio within individual layers do exist, all CRP gathers are analyzed simultaneously. This simultaneous migration and analysis is one advantage of the method presented here since we can migrate with a range of possible Poisson's ratio functions. The Poisson's ratio is solved by using all raypaths in the grided model. The whole model is determined by layer stripping, in a top down procedure. Since Poisson's ratio is related to the velocity ratio (see Figure 4) the term Poisson's ratio and velocity ratio will be used interchangeably in the subsequent sections.

The Method

The traveltime (t_p and t_s) for both P- and S-ray branches from source to receivers are given as the integral along the corresponding ray paths l;

$$t_p = \int_{p_{ray}} \frac{1}{v_p(\mathbf{x})} dl, \tag{1}$$

$$t_s = \int_{s_{ray}} \frac{1}{v_s(\mathbf{x})} dl, \tag{2}$$

where $\mathbf{x}$ is the position vector, dl is the differential distance along the ray. The total traveltime of a ray from the source to the receiver is given as the integral over both slownesses along which the ray traversed to the receiver. The slowness of the medium is made up of the P-wave and S-wave slownesses respectively. Therefore, the total transient time of the ray is given as

$$t_{ps} = \int_{ray_{total}} (1 + v_p(\mathbf{x})/v_s(\mathbf{x})) \frac{1}{v_p(\mathbf{x})} dl \qquad (3)$$

From equation (3) it is seen that the traveltime associated with a given ray (i.e. the total transit time from source to receiver) is the integrated Poisson's ratio along that ray. The difference between the traveltime from a perturbed Poisson's ratio model and an initial model is used to carry out tomographic inversion of Poisson's ratio along the ray path. A difficulty with the tomography problem when using equation (3) is that the ray path itself depends on the unknown Poisson's ratio (note that Poisson's ratio is equivalent to velocity ratio). Therefore equation (3) is non-linear in Poisson's ratio. The approach used here is to linearize equation (3) about some initial or reference Poisson's ratio model. In other words like any tomographic approach, instead of solving equation (3) for $v_p/v_s = \gamma$, we solve some approximation to equation (3) for the perturbation in v_p/v_s from an initial model. The perturbation in traveltime is given in matrix form as:

$$\Delta t_{ps} = \frac{1}{v_p} \Delta \gamma D, \qquad (4)$$

where $\Delta \gamma$ is the vector whose components are the differences in Poisson's ratio between the initial model and the solution, i.e., an (m × 1) vector and D is a matrix whose element D_{ij} is the distance the i-th ray travels in the j-th cell, i.e., an (N × m) matrix and Δt_{ps} is an (N × 1) vector. The symbol N denotes the total number of picked traces, m denotes the total number of model parameters. The matrix D is also given as a matrix whose elements are partial derivatives of the traveltimes with respect to model parameters. In reflection time tomography the model parameters are made up of the total number of cells in the model and the number of reflectors (Bishop et al., 1985). In such a case one has to differentiate the traveltime with respect to the slowness and with respect to the reflector depth. (Bishop et al., 1985) showed that the derivative of the traveltime with respect to the slowness is equal to the path length of the ray in each cell. In the case presented here, since the depth of the reflectors are fixed one would then compute only the traveltime derivative with respect to the Poisson's ratio. Equation (4) is solved using the least-squares formulation of (Paige and Saunders, 1982). This updates the Poisson's ratio model by minimizing the Δt_{ps}. Equation (4) can be used both in prestack or poststack reflection tomography to evaluate changes in reflection traveltime due to changes in v_p/v_s. In the Prestack domain, it will be based on picking, therefore be prone to human or

machine mispicking especially in areas were complex raypaths cause triplications.

To overcome this difficulty the values of Δt_{ps} are computed after the data have been depth migrated and sorted into CRP gathers. Depth deviations (Δz) in migrated CRP gathers are converted to traveltime deviations (traveltime delays Δt_{ps}) along a CRP ray pair. This is done by using the approximate relation between Δz and the resulting ray traveltime deviation (Fara and Madariaga, 1988; Stork, 1992; Kosloff et al., 1996). For a reflecting monotypic ray (e.g P-P):

$$\Delta tpp = 2p_z \Delta z,$$

while:

$$\Delta t_{lm} = \Delta z(p_{zl} + p_{zm}),$$

for polytypic rays of type l and m. The symbol p_z is the vertical slowness component of the incident ray if Δz is the vertical displacement of the boundary level. Substituting for the slowness and taking into account the local dip of the reflector, Δt_{ps} is given as:

$$\Delta t_{ps} = \Delta z \left(\frac{cos(\theta_p - \phi)}{v_p} + \frac{cos(\theta_s + \phi)}{v_s} \right) = \frac{\Delta z}{v_p} \left(cos(\theta_p - \phi) + \frac{v_p}{v_s} cos(\theta_s + \phi) \right), \tag{5}$$

$$v_p \Delta t_{ps} = \Delta z(cos(\theta_p - \phi) + \gamma cos(\theta_s + \phi)) \tag{6}$$

such that Δz is the residual depth deviation, while θ_p and θ_s are the incident and reflection angles at the reflector and ϕ is the local dip of the reflector. This dip is computed from the structure given in the P-wave model.

In equation (4), the i-th row of the D matrix describes the path of the i-th ray from source to receiver. The number of rows equal the total number of rays, whereas the number of columns is equal to the total number of cells (nz × nx) used to describe the model.

The least square solution to equation (4) is given as:

$$\frac{\Delta \gamma}{v_p} = (D^T D + KI)^{-1} D^T \Delta t_{ps}. \tag{7}$$

The constant K (damping factor) added to the main diagonal of matrix $D^T D$ makes D nonsingular and also stabilizes the inversion process (Paige and Saunders, 1982). The solution to equation (4) is a set of Poisson's ratio perturbations $\Delta\gamma$ which are added to the initial Poisson's ratio model to produce an updated model, i.e., the updated Poisson's ratio field is produced by projecting the Δt_{ps} back through the medium over the traced raypaths. At this stage the procedure can be repeated with the updated Poisson's ratio and further updates can be undertaken if the new CRP gathers are not flat enough. It should be noted that, the grid cell to be adjusted are dependent on the raypath associated with their reflection event along which the observations are made. This in turn is dependent on the source and receiver locations of the traces and the overlying Poisson's ratio model. The changes in traveltime that are required in each grid cell translate into changes in the interval Poisson's ratio value of the grid cell.

Equation (3) tells us that when a PS-ray travels through several structures in the earth model, its traveltime is an integral measure of the velocity ratio in the structures that the ray encounters. Unraveling the exact velocity ratio of a structure from travel-time observations is therefore possible only when the structure is penetrated by a large number of rays over a wide range of angles. This means the accuracy of Poisson's ratio analysis by CRP tomography of common shot gathers is best for large source-to-receiver offsets and short shot point separations as well as short separation between CRP-gathers. The initial velocity ratio model can be determined from CRP-semblence velocity ratio analysis, geological information, well logs, or any other source of a priori information.

The algorithm

The procedure follows 5 main steps. Starting at the top layer;

- at locations distributed throughout the model compute depth migrated image gathers at the region of interest, based on an initial Poisson's ratio model,

- estimate the traveltime corrections necessary to flatten the gathers,

- solve a large system of equations to simultaneously obtain the product of P-wave slowness and velocity-ratio updates throughout the model (so-called local tomography),

- divide the product in previous step by the P-wave slowness to obtain the velocity-ratio update,

- add the updated values to the initial values and remigrate. If CRP-flatness is not achieved repeat starting at step 1, if achieved stop.

Synthetic example

To demonstrate the effectiveness of the method described above, a numerical example is presented. Considering the fact that an image depth only depends on the velocity ratio above it, except for turning rays, the use of layer based tomography is applied to determine the Poisson's ratio in individual layers. The model consist of seven elastic layers. The P-wave velocities are 2.075, 2.20, 2.655, 3.00, 4.202, 4.608 and 5.285 km/s while the velocity ratios are 1.5, 1.73, 1.8, 1.73, 1.81, 1.73, 1.73 respectively. The wavelet used is a 30Hz Ricker wavelet with pulse duration of 0.059 s. The synthetic data were computed by a program based on the ray method. For this test a total of 17 shot gathers were generated for a regular receiver grid spacing of 10 m and shot spacing of 100 m with 200 m near offset and 2000 m far offset.

Figure 2 shows a CRP gather at distance $x = 1500$m after migration with a constant velocity-ratio of 1.99. It is diplayed near the velocity model for comparison. Note that the CRP images are curved upward since the Poisson's ratio is higher than the true Poisson's ratio. Thus the S-wave velocity is smaller. Figure 4 shows the relation between Poisson's ratio and shear velocity. This curvature is well displayed in the first layer were the true velocity ratio is 1.5. Image positions in Figure 2 are distorted and will eventually lead to structural distortion of images in the stacked section. The position of the other reflector images eventhough seems to be flatt are moved upward. Compare for example the last two image positions in Figure 2. After an average of seven iterations for each layer-stripping procedure the corrected velocity ratio model is obtained, Figure 3 illustrate the flatness of the common-image gathers despite some migration noise being introduced.

Conclusion

The velocity ratio analysis method presented in this paper can provide a useful tool for determining and updating shear wave velocity models as well as velocity ratios. Together with P-wave velocity and density, some other parameters like elastic impedance, S-wave impedance, P-wave impedance, zero-offset shear-wave reflectivity and Poisson's ratio can be determined. These are important parameters used for lithologic inversion and reservoir characterisation.
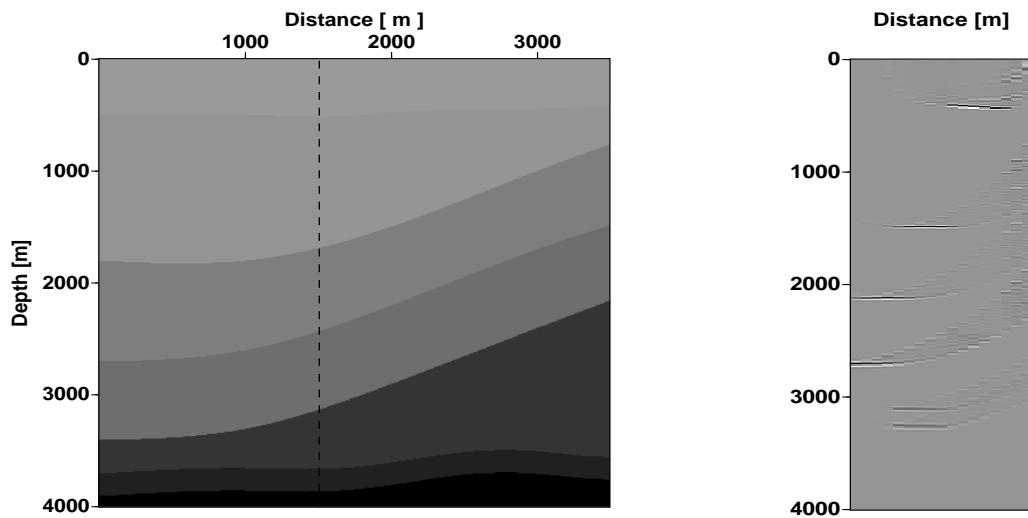
Figure 2: Layered velocity model used in generating common shot gathers. The model is made up of seven layers. The dashed line indicates the imaged position shown on the right panel. This panel is a common image gather at position $x = 1.5$ km with an initial migration v_p/v_s-ratio of 1.99 for the entire model. Using this velocity ratio causes the imaged depths to move upward from their true positions.
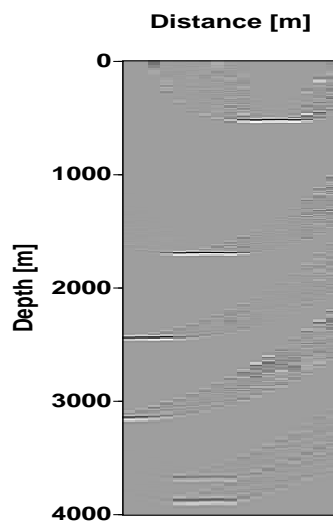

Figure 3: Common image gather from the migrated data with corrected velocity ratio after seven iterations. Displayed is the image gather at position x=1.5 km for comparison with the image gather in Figure 2. Despite some migration noise, the position of the events are correctly imaged.
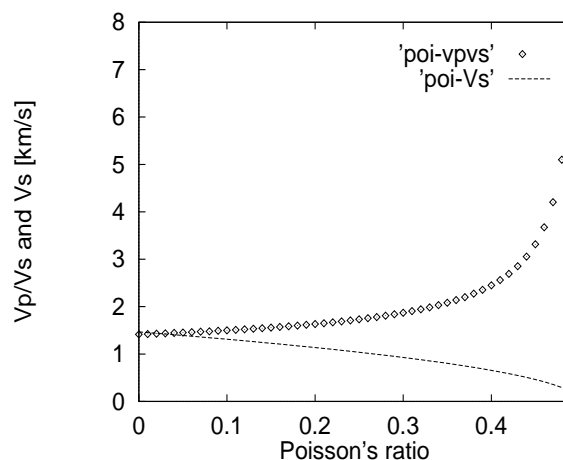
Figure 4: The relationship between Poisson's ratio and v_p/v_s-ratio, and v_s. For a constant P-wave velocity, v_s is inversely proportional to Poisson's ratio

ACKNOWLEDGMENTS

REFERENCES

Al-Yahya, K., 1989, Velocity analysis by iterative profile migration: Geophysics, **54**, 718–729.

Bishop, T. N., Bube, K. P., Cutler, R. T., Langan, R. T., Love, P. L., Resnick, J. R., Shuey, R. T., Spindler, D. A., and Wyld, H. W., 1985, Tomographic determination of velocity and depth in laterally varying media: Geophysics, **50**, 903–923.

Deregowski, S. M., 1990, Common-offset migrations and velocity analysis: First Break, **8**, 225–234.

Fara, V., and Madariaga, R., 1988, Nonlinear reflection: Geophys. J. Internat., **95**, 135–147.

Jeannot, J. P., Faye, J. P., and Denelle, E., 1986, Prestack migration velocities from depth-focusing analysis: 56th Ann. Internat. Mtg., Soc. Expl. Geophys., Expanded Abstracts, pages 438–440.

Kosloff, D., Sherwood, J., Koren, Z., Machet, E., and Kovitz, Y. F., 1996, Velocity and interface depth determination by tomography of depth migrated gathers: Geophysics, **61**, 1511–1523.

Liu, Z., and Bleistein, N., 1995, Migration velocity analysis: Theory and an iterative algorithm: Geophysics, **60**, 142–153.

MacKay, S., and Abma, R., 1992, Imaging and velocity estimation with depth-focusing analysis: Geophysics, **57**, 1608–1622.

Paige, C. C., and Saunders, M. A., 1982, Lsqr: An algorithm for sparse linear equations and sparse least squares: ACM Transactions on Mathematical Software, **8**, 43–71.

Stork, C., 1992, Reflection tomography in the postmigrated domain: Geophysics, **57**, 680–692.